Check for updates

RESEARCH REPORTS
Biological

X. Xu[1,2], C. Chen[2], K. Akiyama[2], Y. Chai[2], A.D. Le[3,4], Z. Wang[1], and S. Shi[2]*

[1]Laboratory of Oral Biomedical Science and Translational Medicine, Tongji University School of Stomatology, Shanghai 200072, China; [2]Center for Craniofacial Molecular Biology, Ostrow School of Dentistry, University of Southern California, 2250 Alcazar Street, CSA 103, Los Angeles, CA 90033, USA; [3]Department of Oral and Maxillofacial Surgery and Pharmacology, Penn Dental Medicine and Penn Medicine Hospital of the University of Pennsylvania, Philadelphia, PA 19104, USA; and [4]The Herman Ostrow School of Dentistry, University of Southern California, Los Angeles, CA 90089, USA; *corresponding author, songtaos@usc.edu

J Dent Res 92(9):825-832, 2013

Gingivae Contain Neural-crest- and Mesoderm-derived Mesenchymal Stem Cells

ABSTRACT

Gingivae represent a unique soft tissue that serves as a biological barrier to cover the oral cavity side of the maxilla and mandible. Recently, the gingivae were identified as containing mesenchymal stem cells (GMSCs). However, it is unknown whether the GMSCs are derived from cranial neural crest cells (CNCC) or the mesoderm. In this study, we show that around 90% of GMSCs are derived from CNCC and 10% from the mesoderm. In comparison with mesoderm MSCs (M-GMSCs), CNCC-derived GMSCs (N-GMSCs) show an elevated capacity to differentiate into neural cells and chondrocytes and induce activated T-cell apoptosis *in vitro*. When transplanted into mice with dextran sulfate sodium (DSS)-induced colitis, N-GMSCs showed superior effects in ameliorating inflammatory-related disease phenotype in comparison with the M-GMSC treatment group. Mechanistically, the increased immunomodulatory effect of N-GMSCs is associated with up-regulated expression of FAS ligand (FASL), a transmembrane protein that plays an important role in MSC-based immunomodulation. In summary, our study indicates that the gingivae contain both neural-crest- and mesoderm-derived MSCs with distinctive stem cell properties.

KEY WORDS: gingiva, mesenchymal stem cells, neural crest cells, differentiation, immunomodulation, apoptosis.

DOI: 10.1177/0022034513497961

Received April 13, 2013; Last revision June 18, 2013; Accepted June 22, 2013

A supplemental appendix to this article is published electronically only at http://jdr.sagepub.com/supplemental.

© International & American Associations for Dental Research

INTRODUCTION

Mesenchymal stem cells possess multipotent differentiation potential and the capability of regulating immune response (Aggarwal and Pittenger, 2005; Nauta and Fibbe, 2007; Uccelli *et al*., 2008), findings which have provided a foundation for the use of MSCs in tissue regeneration and immune therapies (Le Blanc *et al*., 2008; Sun *et al*., 2009; Akiyama *et al*., 2012). The orofacial region contains a variety of distinctive MSC populations, including dental pulp stem cells, stem cells from deciduous dental pulp, periodontal ligament stem cells, apical papilla stem cells, and dental follicle stem cells (Gronthos *et al*., 2000; Miura *et al*., 2003; Seo *et al*., 2004; Morsczeck *et al*., 2005; Yamaza *et al*., 2011). Recently, gingiva/mucosa-derived mesenchymal stem cells (GMSCs) were isolated and characterized as having multi-lineage differentiation capacity and immunomodulatory properties (Zhang *et al*., 2009, 2010; Fournier *et al*., 2010; Marynka-Kalmani *et al*., 2010; Mitrano *et al*., 2010; Su *et al*., 2011; Tang *et al*., 2011). The gingivae represent a unique oral tissue that serves as a biological mucosal barrier to protect the oral cavity side of the maxilla and mandible. Clinically, it is extremely easy to collect gingival tissue by biopsy, and, in the laboratory, it is feasible to isolate GMSCs from gingival tissue based on their highly proliferative nature.

From a developmental point of view, craniofacial mesenchyme is derived from the neural crest and the mesoderm (Driskell *et al*., 2011). Cranial neural crest cells (CNCCs) migrate ventrolaterally as they populate the first branchial arches from the 4-somite stage, giving rise to mesenchymal structures, such as neural tissues, cartilage, bone, and teeth, in the craniofacial region (Chai *et al*., 2000; Chai and Maxson, 2006). Meanwhile, the mesoderm is also involved in orofacial development. A previous study showed that the progenitor cells from the oral mucosa lamina propria may be derived from neural crest cells (Davies *et al*., 2010); however, the composition of the GMSC population is still largely unknown. Since post-migratory CNCCs give rise to most cranial mesenchymal structures, here we used *Wnt1-Cre;R26R* mice to show that most GMSCs are derived from CNCC, along with a small quantity derived from the mesoderm.

MATERIALS & METHODS

Animals

Female C57BL/6J mice and B6.Cg-*Gt(ROSA)26Sor*$^{tm6(CAG-ZsGreen1)Hze}$/J (ZsGreen) mice were purchased from the Jackson Lab (Bar Harbor, ME, USA). The Wnt1-Cre transgenic line and the R26R conditional reporter (*LacZ*) mice were gifts from Dr. Yang Chai's laboratory at the University of Southern California. Mating *Wnt1-Cre*$^{+/-}$ with *R26R*$^{+/+}$ mice generated *Wnt1-Cre;R26R* mice (double transgenic). Mating *Wnt1-Cre*$^{+/-}$ with *ZsGreen*$^{+/+}$ mice generated *Wnt1-Cre;ZsGreen* mice (double transgenic). The mice were used at the age of 8 wks for experiments, under institutionally approved protocols for the use of animals in research (University of Southern California #10941 and 11141).

Antibodies and Reagents

All antibodies and reagents used in this study are described in the Appendix.

Cell Cultures

GMSCs from *Wnt1-Cre;R26R* mice and *Wnt1-Cre;ZsGreen* mice were cultured as described in the Appendix.

Colony-forming Units-Fibroblastic (CFU-F) Assay

CFU-F assay was performed as described in the Appendix.

Detection of β-galactosidase (lacZ) Activities by X-gal Staining

Detailed methods for X-gal staining are described in the Appendix.

Proliferation Assay

Proliferation rates of GMSCs were assessed by the use of a bromodeoxyuridine (BrdU) staining kit (Invitrogen, Carlsbad, CA, USA), according to the manufacturer's protocols.

Population Doublings (PD)

The detailed method for PD is described in the Appendix.

Cell Sorting

GMSCs from *Wnt1-Cre;ZsGreen* mice at passage 2 (P2) were trypsinized and washed in PBS supplemented with 2% heat-inhibited FBS. Cells were then transferred to a 5-mL polystyrene tube (Falcon, Franklin Lakes, NJ, USA) and applied through FACSAria II (BD Biosciences, San Jose, CA, USA). All FITC-positive cells were collected as N-GMSCs, while the FITC-negative cells were collected as M-GMSCs.

Flow Cytometric Analysis

Detailed methods are described in the Appendix.

Real-time PCR

Real-time PCR was performed as described in the Appendix.

Immunofluorescence and Immunohistochemistry Staining

Immunofluorescence and immunohistochemistry staining were performed as described in the Appendix.

Multi-lineage Differentiation Assay

For *in vitro* differentiation assay, P2 GMSCs were cultured under osteogenic, adipogenic, chondrogenic, and neurogenic conditions, as described in the Appendix.

Western Blot Analysis

Western blot was performed as described in the Appendix.

FASL Knockdown

To knock down FASL expression, we seeded 2×10^5 GMSCs in a 12-well culture plate. *Fasl* siRNA (Santa Cruz Biotechnology, Santa Cruz, CA, USA) was used according to the manufacturer's protocols.

Co-culture of GMSCs with Activated Splenocytes

Co-culture of GMSCs with activated splenocytes was performed as described in the Appendix.

Dextran Sulfate Sodium (DSS)-induced Mouse Colitis and Treatment with GMSCs

Acute colitis was induced in C57BL/6J mice. The detailed methods are described in the Appendix. For GMSC treatment, 2×10^5 of P2 GMSCs were infused intravenously into mice with colitis (n = 5 each group) at 3 days post-DSS induction. All mice were euthanized at day 10 and analyzed as previously described (Alex *et al*., 2009). The results are representative of 3 independent experiments.

Statistics

SPSS 13.0 was used to perform statistical analysis. Significance was assessed by independent two-tailed Student's *t* test or analysis of variance (ANOVA). *p* values less than .05 were considered as significant.

RESULTS

Characterization of N-GMSCs and M-GMSCs

X-gal staining showed that the gingival mesenchyme of *Wnt1-Cre; R26R (LacZ)* mice contained CNCC-derived β-galactosidase-positive cells and mesoderm-derived β-galactosidase-negative, but Nuclear Fast Red–positive, cells (Fig. 1A). When EdU was injected (i.p.) into *Wnt1-Cre; Zsgreen* mice for 7 days and traced for 2 wks, the majority of EdU^+ cells co-localized with the

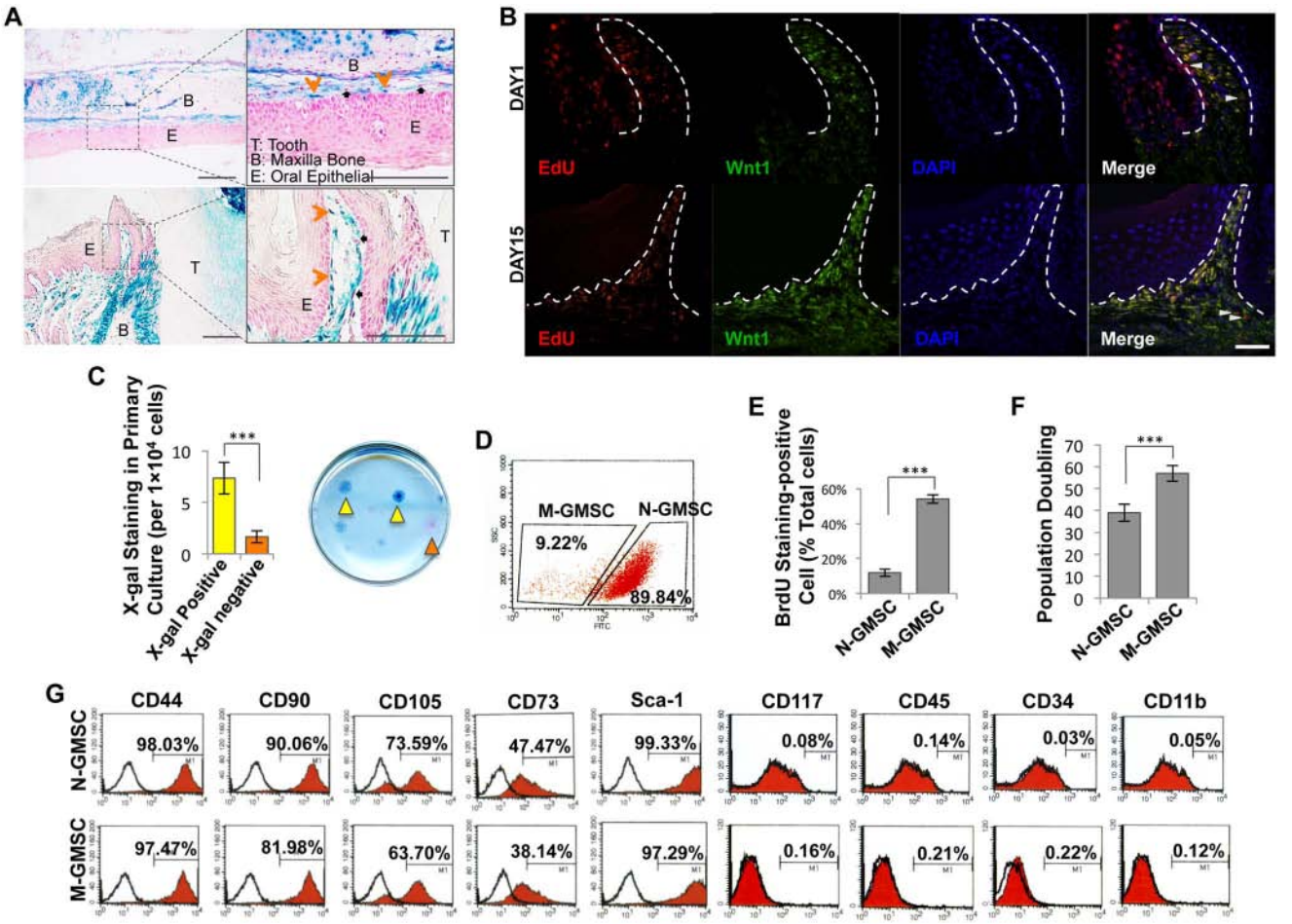

Figure 1. Characterization of N-GMSCs and M-GMSCs. (**A**) X-gal staining showed that gingivae contained neural-crest-cell-derived blue cells (orange arrows) and mesoderm-derived red cells (black arrows; T, Tooth; B, Bone; E, Epithelial; scale bar = 100 μm). (**B**) Injection (i.p.) of EdU (500 μg in 200 μL) into 4-week-old *Wnt1-Cre;Zsgreen* mice. Maxillary samples were harvested on Day 1 and Day 15 post-EdU injection. The majority of the EdU$^+$ cells (red) co-localized with the Zsgreen$^+$ neural-crest-derived cells (green). Some EdU$^+$ cells failed to co-localize with neural crest cells (white triangle). (White dotted line = epithelial basement line; scale bar = 100 μm.) (**C**) Single-colony assay showed neural crest origin N-GMSCs (blue, yellow arrows) and M-GMSCs (red, orange arrows) (n = 5). (**D**) N-GMSCs (FITC-positive) and M-GMSCs (FITC-negative) were isolated from *Wnt1-Cre;Zsgreen* mice by flow cytometry. (**E**) Proliferation rate of cultured GMSCs was assessed by BrdU incorporation assay for 24 hrs. The number of BrdU-positive cells was indicated as a percentage of the total number of counted GMSCs and averaged from 5 replicated cultures (n = 5). (**F**) Continued culture assay showed that M-GMSCs had more elevated population doublings than N-GMSCs (n = 3). (**G**) Flow cytometric analysis showed that both N-GMSCs and M-GMSCs were positive for the surface molecules CD 44, CD90, CD 105, CD73, and Sca-1, while they failed to express CD34, CD45, CD117, and CD11b. Error bars represent mean ± SD; ***$p < .001$.

Zsgreen$^+$ neural-crest-derived cells. Some EdU$^+$ cells failed to co-localize with neural crest cells (white triangle) (Fig. 1B). When MSCs were isolated from the gingiva and cultured at a low density, most adherent single-colony clusters were found to be β-galactosidase-positive N-GMSCs, with fewer β-galactosidase-negative M-GMSCs clusters (Fig. 1C). Next, we used *Wnt1-Cre;Zsgreen* mice, in which CNCC-derived cells continuously express ZsGreen protein and are FITC-positive under flow cytometric analysis, to separate N-GMSCs and M-GMSCs accurately. We found that around 90% of single-colony-derived GMSCs were N-GMSCs, while 10% were M-GMSCs (Fig. 1D). We demonstrated that M-GMSCs showed an elevated cell proliferation rate and population doubling, as determined by BrdU incorporation and continued culture assays, respectively, when compared with N-GMSCs (Figs. 1E, 1F). Flow cytometric analysis confirmed that both N-GMSCs and M-GMSCs were positive for the mesenchymal stem cell surface markers CD44, CD90, CD105, CD73, and Sca-1, but were negative for the hematological markers CD117, CD45, and CD34 and the macrophage marker CD11b (Fig. 1G).

Multi-lineage Differentiation of N-GMSCs and M-GMSCs

Under osteogenic culture conditions, N-GMSCs and M-GMSCs showed the same capability to form mineralized nodules (Appendix Fig. 1A), as assessed by Alizarin Red staining, and expressed the osteogenic markers alkaline phosphatase (ALP), osteocalcin (OCN), and runt-related transcription factor 2 (RUNX2), as determined by Western blot analysis (Figs. 2A, 2B). Also, N-GMSCs and M-GMSCs had the same adipogenic

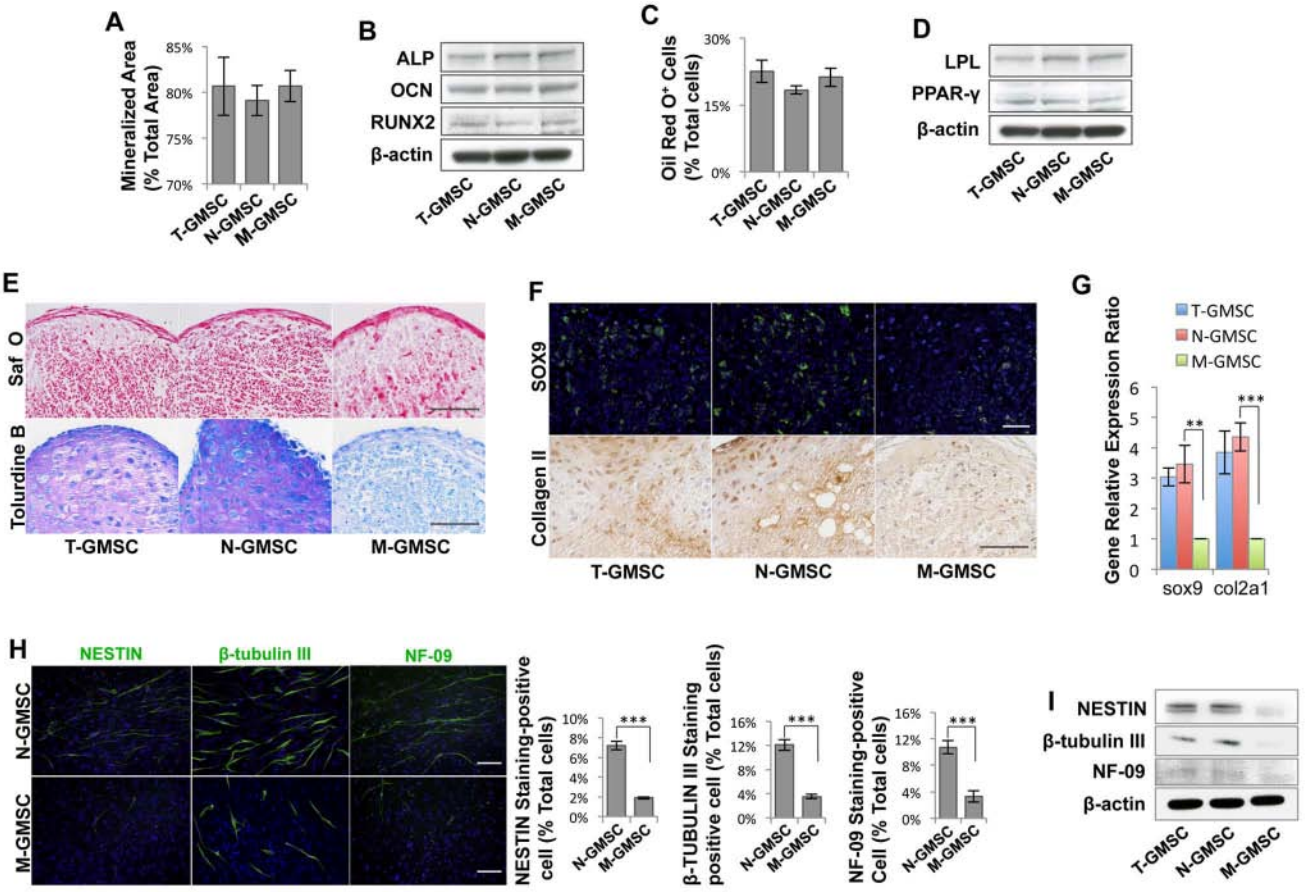

Figure 2. Multi-lineage differentiation of N-GMSCs and M-GMSCs. (**A**) Semi-quantitative analysis of the percentage of alizarin-red-stained mineralized area *vs.* total area after cultured in osteoinductive conditions for 4 wks indicated that there was no significant difference between N-GMSCs and M-GMSCs in the formation of mineralized nodules. (**B**) Western blot analysis confirmed that N-GMSCs and M-GMSCs expressed the same levels of the osteogenic genes ALP, RUNX2, and OCN. (**C**) No significant difference was seen between N-GMSCs and M-GMSCs in the formation of Oil red O-positive adipocytes after culture in adipo-inductive conditions for 2 wks. (**D**) Western blot analysis confirmed that N-GMSCs and M-GMSCs expressed similar levels of the adipogenic markers PPARγ-2 and LPL. (**E**) Cell pellets derived from *in vitro* chondrogenic culture were sectioned and stained with safranin-O or toluidine blue. N-GMSCs showed more safranin-O- and toluidine-blue-positive areas than in the M-GMSC group. (**F**) Immunofluorescence staining showed that N-GMSCs expressed a high level of SOX-9-positive cells when compared with M-GMSCs. Immunohistochemistry staining also showed stronger COLLAGEN II expression in the N-GMSC group. (**G**) Real-time PCR identified that N-GMSCs expressed higher sox9 and collagen II on the gene level when compared with M-GMSCs. (**H**) After N-GMSC culture in the neural differentiation media for 21 days, immunocytostaining showed a significantly elevated expression of neurofilament M (NF-09), β-TUBULIN III, and NESTIN when compared with M-GMSCs (n = 5). (**I**) Western blot analysis confirmed that N-GMSCs expressed higher levels of neurogenesis protein NF-09, β-TUBULIN III, and NESTIN compared with M-GMSCs. $^{**}p < .01$, $^{***}p < .001$; Error bars: mean ± SD. Scale bar = 100 μm.

differentiation potential, as assessed by Oil red O-positive staining (Appendix Fig. 1B) to show the number of adipocytes, and by Western blot to show the expression of the adipocyte-specific transcripts peroxisome proliferator-activated receptor γ (PPARγ) and lipoprotein lipase (LPL) (Figs. 2C, 2D). To assess chondrogenic capacity, we cultured N-GSMCs and M-GMSCs in chondrogenic induction media for 4 wks. Safranin-O and toluidine blue staining showed that N-GMSCs generated more cartilage matrix than M-GSMCs (Fig. 2E). Additionally, immunofluorescence and immunohistochemistry staining showed that N-GMSCs express a high level of the chondrogenic marker SOX9 and Collagen II compared with M-GMSCs (Fig. 2F). Real-time PCR identified that N-GMSCs expressed higher sox9 and collagen II on the transcriptional level when compared with M-GMSCs (Fig. 2G).

Since the N-GMSCs were derived from CNCCs, we examined the neural differentiation potential of N-GMSCs and discovered that N-GMSCs showed significantly elevated expression of neural markers, including neurofilament M (NF-09), β-TUBULIN III, and NESTIN, when cultured under neural induction conditions for 3 wks, in comparison with M-GSMCs (Fig. 2H). Western blot analysis confirmed that N-GMSCs expressed higher levels of neurofilament M (NF-09), β-TUBULIN III, and NESTIN when compared with M-GMSCs (Fig. 2I).

Immunomodulatory Property of GMSCs

Since GMSCs possess an immunomodulatory property (Zhang *et al.*, 2009), here we compared immunotherapeutic effects

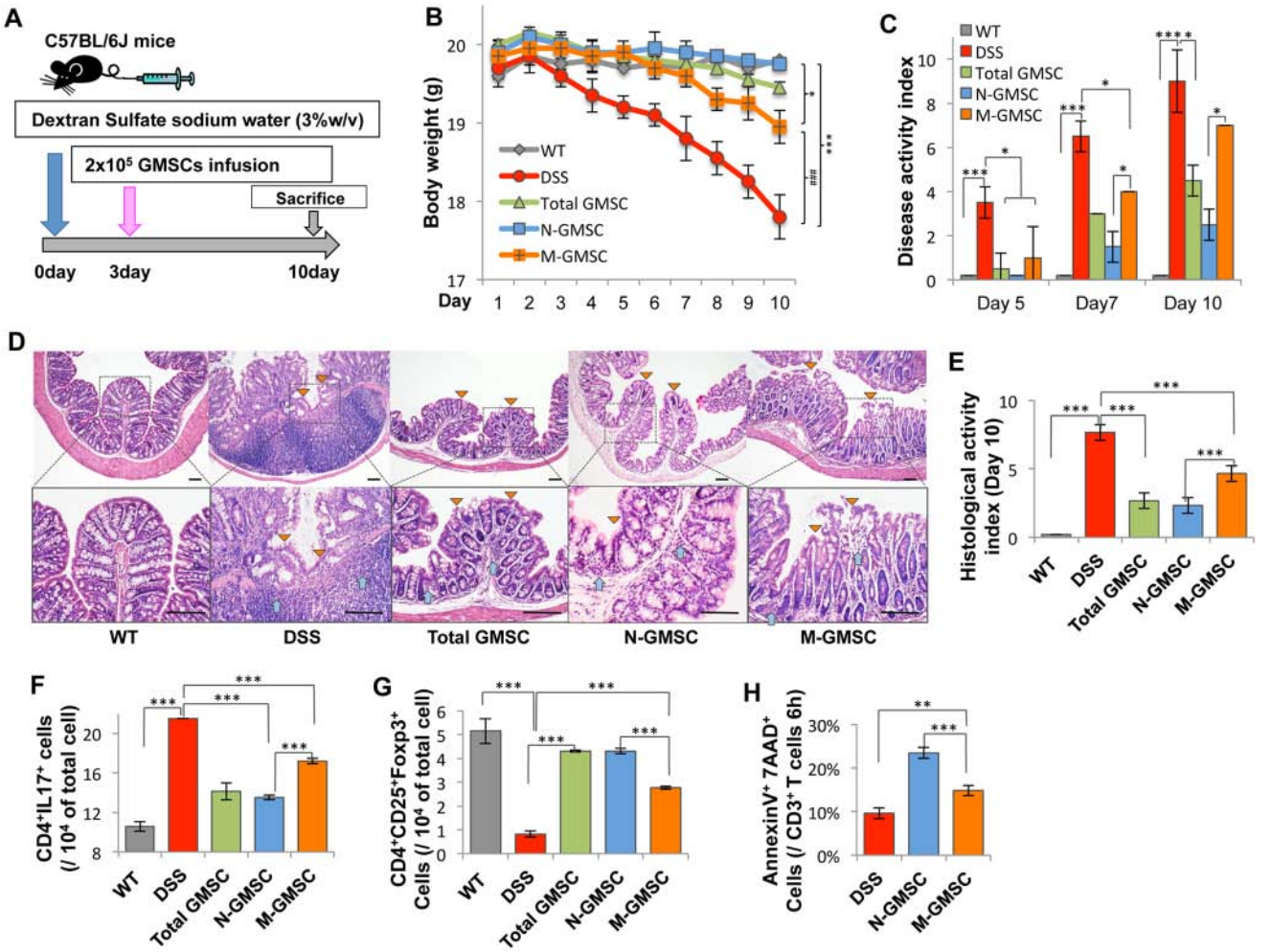

Figure 3. N-GMSCs can ameliorate disease phenotype in dextran sulfate sodium (DSS)-induced experimental colitis. (**A**) Schema showing GMSC infusion in mice with DSS-induced experimental colitis. (**B**) Mice with colitis (colitis, n = 5) showed significantly reduced body weight from days 5 to 10 after DSS induction. N-GMSC (n = 5), M-GMSC (n = 5), and total GMSC (T-GMSC, n = 5) transplantation reduced body weight loss compared with that of the colitis group (n = 5) at 10 days post-DSS induction. However, the N-GMSC and T-GMSC groups showed more significant reduction of body weight loss than did the M-GMSC group (*$p < .05$ *vs.* C57BL/6J; ***$p < .001$ *vs.* C57BL/6J; ###$p < .001$ *vs.* M-GMSCs). (**C**) Disease activity index (DAI) was significantly increased in mice with colitis compared with the C57BL/6J control mice (n = 5) from days 5 to 10 post-DSS induction. Although all GMSC infusion groups showed significantly reduced DAI scores, the N-GMSC and T-GMSC groups demonstrated superior reduction when compared with the M-GMSC group. (**D**) Hematoxylin and eosin (H&E) staining showed the infiltration of inflammatory cells (blue arrows) in the colon, with destruction of the epithelial layer (yellow triangles) in mice with colitis. N-GMSC transplantation exerted more significant restoration of disease phenotype in the colon and reduction of histological activity index (**E**) compared with those in the M-GMSC group. (**F**) The Th17 cell level was significantly elevated in mice with colitis compared with C57BL/6J control mice at 10 days post-DSS induction. Compared with the M-GMSC group, N-GMSC infusion showed a significant effect in reducing the levels of Th17 cells in mice with colitis at 10 days post-DSS induction. (**G**) Treg level was significantly reduced in mice with colitis compared with C57BL/6J control mice at 10 days post-DSS induction. N-GMSC infusion exhibited stronger capacity to up-regulate the Treg levels in mice with colitis compared with the M-GMSC group. (**H**) By flow cytometric analysis, N-GMSC (n = 3) infusion showed marked elevation in the number of apoptotic $CD3^+$ T-cells compared with those in the M-GMSC group at 6 hrs post-infusion in mice with colitis. Scale bar = 200 μm; *$p < .05$; **$p < .01$; ***$p < .001$. Error bars: mean ± SD.

between N-GMSCs and M-GSMCs in mice with dextran sulfate sodium (DSS)-induced experimental colitis (Alex *et al*., 2009). N-GMSCs or M-GMSCs (2×10^5) sorted by flow cytometry were systemically transplanted into mice with experimental colitis at day 3 after 3% DSS treatment (Fig. 3A). The body weight of mice with colitis was significantly reduced when compared with that of the control C57BL/6J mice (Fig. 3B). Although infusion of both N-GMSC and M-GMSC could partially restore reduced body weight in mice with DDS-induced colitis, N-GMSCs showed more significant restoration of reduced body weight compared with M-GMSCs (Fig. 3B). The disease activity index (DAI), including body weight loss, diarrhea, and bleeding, was significantly elevated in the mice with colitis compared with the control group. After N-GMSC and M-GMSC infusion, the DAI score was decreased. However, N-GMSC infusion induced a more significant reduction in the DAI score than in that of the M-GMSC group from 5-10 days post-GMSC infusion (Fig. 3C). Colon tissues from each group

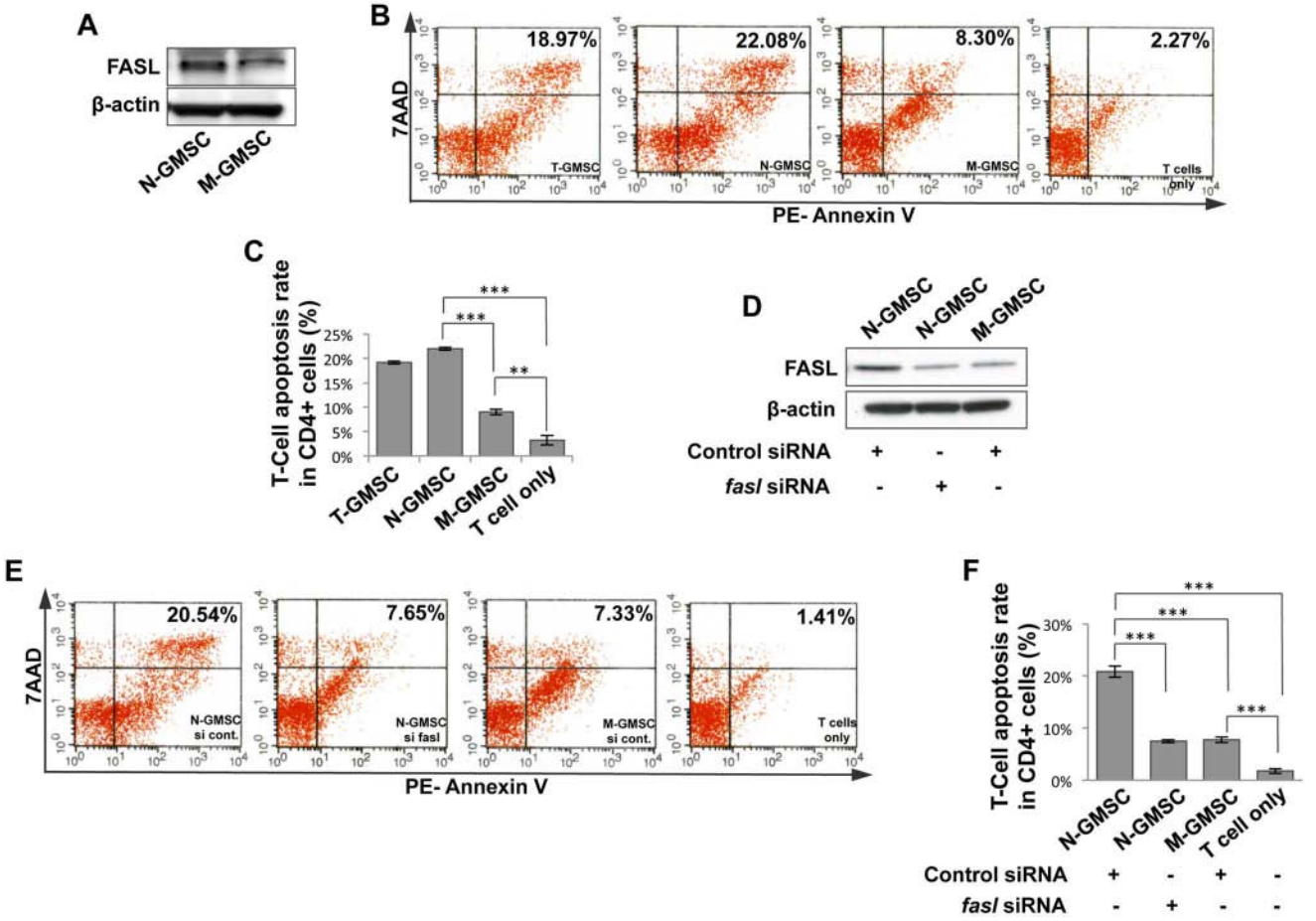

Figure 4. N-GMSCs require FASL to maintain elevated immunomodulatory function. (**A**) Western blot analysis showed that N-GMSCs expressed elevated levels of FASL compared with M-GMSCs. (**B, C**) When co-cultured with T-cells, N-GMSCs showed an elevated capacity to inhibit T-cell viability when compared with M-GMSCs. Apoptosis assay confirmed that N-GMSCs more effectively induced 7AAD/Annexin-positive apoptotic T-cells when compared with the M-GMSC group. (**D**) Western blot analysis showed efficacy of knockdown of *fasl* expression by siRNA in N-GMSCs. (**E, F**) When co-cultured with T-cells, apoptosis assay confirmed that FASL knockdown N-GMSCs resulted in a reduced capacity to induce 7AAD/Annexin-positive apoptotic T-cells when compared with the control siRNA group. $^{**}p < .01$; $^{***}p < .001$; n = 3. Error bars: mean ± SD.

were analyzed by histological section. Absence of an epithelial layer and infiltration of inflammatory cells were observed in the mice with colitis, but infusion of either N-GMSC or M-GMSC restored impaired histological structures (Fig. 3D, Appendix Fig. 3). Compared with the M-GMSC group, however, the N-GMSC group had superior histological recovery of the epithelial structure (yellow triangle) and elimination of inflammatory cells (blue arrow) in the mice with colitis, as assessed by the histological activity index (Fig. 3E), which included ameliorating colonic transmural inflammation, reducing wall thickness, suppressing epithelial ulceration, and restoring normal intestinal architecture. Reduced Tregs and elevated Th17 cells were observed in the mice with colitis at day 10 post-DSS induction (Figs. 3F, 3G). Both N-GMSC and M-GMSC transplantation up-regulated Treg levels, but down-regulated the levels of Th17 cells. However, the N-GMSC group showed more significant up-regulation of Tregs and down-regulation of Th17 cells when compared with the M-GMSC group (Figs. 3F, 3G). A previous study indicated that mesenchymal stem-cell-induced T-cell apoptosis could trigger macrophages to produce high levels of TGFβ, which, in turn, led to the up-regulation of $CD4^+CD25^+$ $Foxp3^+$ Tregs to result in immune tolerance (Akiyama *et al*., 2012). Here we revealed that N-GMSC transplantation induced more marked T-cell apoptosis than that achieved by the M-GMSC group (Fig. 3H).

N-GMSC-mediated Immunomodulation is Associated with Elevated Expression of Fas Ligand (FASL)

Since FASL plays an important role in mesenchymal stem-cell-induced immune tolerance (Yamaza *et al*., 2010; Akiyama *et al*., 2012), we hypothesized that FASL might contribute to the enhanced immunoregulatory function of N-GMSCs. To test this hypothesis, we demonstrated that N-GMSCs expressed an elevated level of FASL compared with M-GMSCs (Fig. 4A). To confirm that FASL expression was correlated with elevated immunomodulatory capacity in N-GMSCs, we first showed that N-GMSCs had significantly elevated capacity to induce

activated T-cell apoptosis in an *in vitro* co-culture system when compared with M-GMSCs (Figs. 4B, 4C). Then we used the siRNA approach to knock down FASL expression in N-GMSCs (Fig. 4D) and found that the capacity to induce activated T-cell apoptosis by fasL siRNA-treated N-GMSCs was significantly reduced (Figs. 4E, 4F). With systemic infusion of GFP^+ GMSCs, GFP^+ cells reached the peak in peripheral blood at 1.5 hrs post-infusion, and became undetectable at 24 hrs (Appendix Fig. 2A), while GFP^+ apoptotic cells reached the peak at 6 hrs post-infusion and became undetectable at 24 hrs post-infusion in peripheral blood (Appendix Fig. 2B). Immunostaining showed that only a few GFP^+ cells were detected in the lung, but not in the liver, spleen, kidney, and colon, at 24 hrs post-infusion, as assessed in multiple tissue sections (Appendix Fig. 2C). Analysis of these data suggests that homing of infused GMSCs may not play a major role in GMSC-mediated therapy in mice with colitis.

DISCUSSION

The vertebrate neural crest cell (NCC) is a multipotent cell population derived from the lateral ridges of the neural plate and gives rise to multiple types of derivatives (Bronner-Fraser and Fraser, 1988). Some post-migratory NCCs also possess the capacity for self-renewal and multipotent differentiation (Lo and Anderson, 1995; Chung *et al*., 2009). In this study, we first demonstrated that both NCC-derived stem cells and non-NCC-derived mesoderm stem cells reside in gingival mesenchyme. A previous study showed that X-gal-positive cells were found in the gingival area of *Mesp1-Cre;R26R* mice, suggesting that mesoderm-derived cells may contribute to gingivae formation (Rothová *et al*., 2011).

Although N-GMSCs and M-GMSCs showed some identical stem cell properties, such as expression of mesenchymal stem cell surface markers and multipotent differentiation, they also exhibited distinctive characteristics. N-GMSCs have a significantly increased capacity to differentiate into neural cells when cultured under neural differentiation conditions, suggesting their potential for use in neural tissue regeneration. Also, N-GMSCs have a greater potential to differentiate into chondrocytes when compared with M-GMSCs. Although the detailed mechanism of N-GMSC-associated chondrogenic differentiation is unknown, the use of N-GMSCs for cartilage repair might be an optimal approach, especially for temporomandibular joint cartilage, which was originally developed from neural crest cells (Chai *et al*., 2000).

T-cells were divided into Th1, Th2, or Th17 cells, depending on the cytokines they produce. Th17 cells produce IL-17, IL-17F, and IL-22, and thereby are capable of clearing pathogens during host defense reactions and inducing tissue inflammation in autoimmune disease. The participation of TGF-beta in the differentiation of Th17 cells places the Th17 lineage in a close relationship to $CD4^+CD25^+Foxp3^+$ regulatory T-cells (Tregs), since TGF-beta also induces differentiation of naïve T-cells into $Foxp3^+$ Tregs in the peripheral immune compartment. Exaggerated Th17 responses have also been observed in animal models of colitis (Ostanin *et al*., 2009). The development of colitis has been associated with an imbalance between pro-inflammatory effector Th17 cells and anti-inflammatory Treg subsets in inflamed mucosa. In this study, N-GMSCs showed an elevated capacity to ameliorate disease phenotype in mice with DSS-induced colitis by the highly expressed FASL, which induced activated T-cell apoptosis and eventually results in immune tolerance. The FASL/FAS pathway is an important cell death pathway in many cell types (O'Reilly *et al*., 2009). Our previous study indicated that mesenchymal stem-cell-induced immune tolerance was associated with FASL-triggered T-cell apoptosis *via* the FAS pathway, and that macrophages subsequently took apoptotic T-cells to release a high level of TGFβ-regulated Tregs (Akiyama *et al*., 2012). Here, we revealed that N-GMSCs possess superior immunoregulatory function by expression of a high level of FASL. Conversely, knockdown of FASL in N-GMSCs showed a significant reduction in their immunoregulatory capacity.

The craniofacial facial region undergoes a unique developmental process compared with other parts of the body. Interplay between and among cells from different tissue layers may contribute to tissue development and formation. A previous study showed a dual origin for epithelium of the middle ear (Thompson *et al*., 2013). Here we identify the difference between N-GMSCs and M-GMSCs in gingiva, suggesting that further investigations are required to understand the interaction between them in terms of their functional roles in gingival immune defense and wound healing.

In summary, this study showed, for the first time, that GMSCs contain neural-crest-derived N-GMSCs and mesoderm-derived M-GMSCs. In comparison with M-GMSCs, N-GMSCs show an increased capacity to differentiate to neural cells and chondrocytes, as well as to modulate immune cells.

ACKNOWLEDGMENTS

This work was supported by grants from the U.S. National Institute of Dental and Craniofacial Research, National Institutes of Health, Department of Health and Human Services (R01DE017449 and R01DE019932 to S.S.). The authors declare no potential conflicts of interest with respect to the authorship and/or publication of this article.

REFERENCES

Aggarwal S, Pittenger MF (2005). Human mesenchymal stem cells modulate allogeneic immune cell responses. *Blood* 105:1815-1822.

Akiyama K, Chen C, Wang D, Xu X, Qu C, Yamaza T, *et al*. (2012). Mesenchymal-stem-cell-induced immunoregulation involves FAS-ligand-/FAS-mediated T cell apoptosis. *Cell Stem Cell* 10:544-555.

Alex P, Zachos NC, Nguyen T, Gonzales L, Chen TE, Conklin LS, *et al*. (2009). Distinct cytokine patterns identified from multiplex profiles of murine DSS and TNBS-induced colitis. *Inflamm Bowel Dis* 15:341-352.

Bronner-Fraser M, Fraser SE (1988). Cell lineage analysis reveals multipotency of some avian neural crest cells. *Nature* 335:161-164.

Chai Y, Maxson RE Jr (2006). Recent advances in craniofacial morphogenesis. *Dev Dyn* 235:2353-2375.

Chai Y, Jiang X, Ito Y, Bringas P Jr, Han J, Rowitch DH, *et al*. (2000). Fate of the mammalian cranial neural crest during tooth and mandibular morphogenesis. *Development* 127:1671-1679.

Chung IH, Yamaza T, Zhao H, Choung PH, Shi S, Chai Y (2009). Stem cell property of postmigratory cranial neural crest cells and their utility in alveolar bone regeneration and tooth development. *Stem Cells* 27:866-877.

Davies LC, Locke M, Webb RD, Roberts JT, Langley M, Thomas DW, *et al*. (2010). A multipotent neural crest-derived progenitor cell population is resident within the oral mucosa lamina propria. *Stem Cells Dev* 19:819-830.

Driskell RR, Clavel C, Rendl M, Watt FM (2011). Hair follicle dermal papilla cells at a glance. *J Cell Sci* 124(Pt 8):1179-1182.

Fournier BP, Ferre FC, Couty L, Lataillade JJ, Gourven M, Naveau A, *et al*. (2010). Multipotent progenitor cells in gingival connective tissue. *Tissue Eng Part A* 16:2891-2899.

Gronthos S, Mankani M, Brahim J, Robey PG, Shi S (2000). Postnatal human dental pulp stem cells (DPSCs) *in vitro* and *in vivo*. *Proc Natl Acad Sci USA* 97:13625-13630.

Le Blanc K, Frassoni F, Ball L, Locatelli F, Roelofs H, Lewis I, *et al*. (2008). Mesenchymal stem cells for treatment of steroid-resistant, severe, acute graft-versus-host disease: a phase II study. *Lancet* 371:1579-1586.

Lo L, Anderson DJ (1995). Postmigratory neural crest cells expressing c-RET display restricted developmental and proliferative capacities. *Neuron* 15:527-539.

Marynka-Kalmani K, Treves S, Yafee M, Rachima H, Gafni Y, Cohen MA, *et al*. (2010). The lamina propria of adult human oral mucosa harbors a novel stem cell population. *Stem Cells* 28:984-995.

Mitrano TI, Grob MS, Carrion F, Nova-Lamperti E, Luz PA, Fierro FS, *et al*. (2010). Culture and characterization of mesenchymal stem cells from human gingival tissue. *J Periodontol* 81:917-925.

Miura M, Gronthos S, Zhao M, Lu B, Fisher LW, Robey PG, *et al*. (2003). SHED: stem cells from human exfoliated deciduous teeth. *Proc Natl Acad Sci USA* 100:5807-5812.

Morsczeck C, Götz W, Schierholz J, Zeilhofer F, Kühn U, Möhl C, *et al*. (2005). Isolation of precursor cells (PCs) from human dental follicle of wisdom teeth. *Matrix Biol* 24:155-165.

Nauta AJ, Fibbe WE (2007) .Immunomodulatory properties of mesenchymal stromal cells. *Blood* 110:3499-3506

O'Reilly LA, Tai L, Lee L, Kruse EA, Grabow S, Fairlie WD, *et al*. (2009). Membrane-bound Fas ligand only is essential for Fas-induced apoptosis. *Nature* 461:659-663.

Ostanin DV, Bao J, Koboziev I, Gray L, Robinson-Jackson SA, Kosloski-Davidson M, *et al*. (2009). T cell transfer model of chronic colitis: concepts, considerations, and tricks of the trade. *Am J Physiol Gastrointest Liver Physiol* 296:G135-146.

Rothová M, Feng J, Sharpe PT, Peterková R, Tucker AS (2011). Contribution of mesoderm to the developing dental papilla. *Int J Dev Biol* 55:59-64.

Seo BM, Miura M, Gronthos S, Bartold PM, Batouli S, Brahim J, *et al*. (2004). Investigation of multipotent postnatal stem cells from human periodontal ligament. *Lancet* 364:149-155.

Su WR, Zhang QZ, Shi SH, Nguyen AL, Le AD (2011). Human gingiva-derived mesenchymal stromal cells attenuate contact hypersensitivity via prostaglandin E(2)-dependent mechanisms. *Stem Cells* 29:1849-1860.

Sun L, Akiyama K, Zhang H, Yamaza T, Hou Y, Zhao S, *et al*. (2009). Mesenchymal stem cell transplantation reverses multiorgan dysfunction in systemic lupus erythematosus mice and humans. *Stem Cells* 27:1421-1432.

Tang L, Li N, Xie H, Jin Y (2011). Characterization of mesenchymal stem cells from human normal and hyperplastic gingiva. *J Cell Physiol* 226:832-842.

Thompson H, Tucker AS (2013). Dual origin of the epithelium of the mammalian middle ear. *Science* 339:1453-1456.

Uccelli A, Moretta L, Pistoia V (2008). Mesenchymal stem cells in health and disease. *Nat Rev Immunol* 8:726-736.

Yamaza T, Kentaro A, Chen C, Liu Y, Shi Y, Gronthos S, *et al*. (2010). Immunomodulatory properties of stem cells from human exfoliated deciduous teeth. *Stem Cell Res Ther* 1:5.

Yamaza T, Ren G, Akiyama K, Chen C, Shi Y, Shi S (2011). Mouse mandible contains distinctive mesenchymal stem cells. *J Dent Res* 90:317-324.

Zhang Q, Shi S, Liu Y, Uyanne J, Shi Y, Shi S, *et al*. (2009). Mesenchymal stem cells derived from human gingiva are capable of immunomodulatory functions and ameliorate inflammation-related tissue destruction in experimental colitis. *J Immunol* 183:7787-7798.

Zhang Q, Su WR, Shi SH, Wilder-Smith P, Xiang AP, Wong A, *et al*. (2010). Human gingiva-derived mesenchymal stem cells elicit polarization of m2 macrophages and enhance cutaneous wound healing. *Stem Cells* 28:1856-1868.